A multilayer electro-thermal model of pouch battery during normal discharge and internal short circuit process

Chen, Mingbiao; Bai, Fanfei; Song, Wenji; Lv, Jie; Lin, Shili; Feng, Ziping; Li, Yongliang; Ding, Yulong

DOI:
10.1016/j.applthermaleng.2017.03.135

Document Version
Peer reviewed version

Citation for published version (Harvard):
Chen, M, Bai, F, Song, W, Lv, J, Lin, S, Feng, Z, Li, Y & Ding, Y 2017, 'A multilayer electro-thermal model of pouch battery during normal discharge and internal short circuit process', *Applied Thermal Engineering*, vol. 120, pp. 506-516. https://doi.org/10.1016/j.applthermaleng.2017.03.135

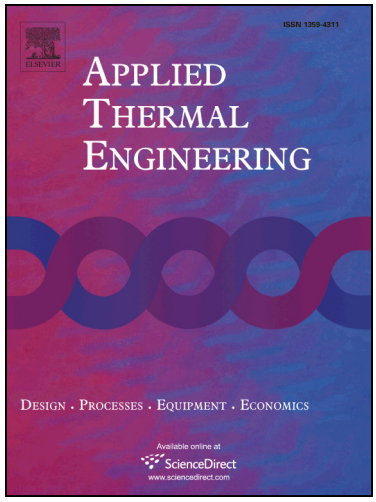

Research Paper

A multilayer electro-thermal model of pouch battery during normal discharge and internal short circuit process

Mingbiao Chen, Fanfei Bai, Wenji Song, Jie Lv, Shili Lin, Ziping Feng, Yongliang Li, Yulong Ding

PII: S1359-4311(16)32532-7
DOI: http://dx.doi.org/10.1016/j.applthermaleng.2017.03.135
Reference: ATE 10139

To appear in: *Applied Thermal Engineering*

Received Date: 18 October 2016
Revised Date: 27 March 2017
Accepted Date: 31 March 2017

Please cite this article as: M. Chen, F. Bai, W. Song, J. Lv, S. Lin, Z. Feng, Y. Li, Y. Ding, A multilayer electro-thermal model of pouch battery during normal discharge and internal short circuit process, *Applied Thermal Engineering* (2017), doi: http://dx.doi.org/10.1016/j.applthermaleng.2017.03.135

A multilayer electro-thermal model of pouch battery during normal discharge and internal short circuit process

Mingbiao Chen,[a,b,c] Fanfei Bai,[a,b,c,d] Wenji Song,[a,b,c]* Jie Lv,[a,b,c] Shili Lin,[a,b,c] Ziping Feng[a,b,c] , Yongliang Li,[e] Yulong Ding,[e]

[a]Guangzhou Institute of Energy Conversion, Chinese Academy of Sciences, Guangzhou 510640, China

[b]Key Laboratory of Renewable Energy, Chinese Academy of Sciences, Guangzhou 510640, China

[c]Guangdong Provincial Key Laboratory of New and Renewable Energy Research and Development, Guangzhou 510640, China

[d]University of Chinese Academy of Sciences, Beijing 10049, China

[e]School of Chemical Engineering, University of Birmingham, Birmingham B152TT, United Kingdom

The following is the e-mail of authors.:

1) Name: Mingbiao Chen E-mail: chenmb@ms.giec.ac.cn

2) Name: Fanfei Bai E-mail: baiff@ms.giec.ac.cn

3) Name: Wenji Song* E-mail: songwj@ms.giec.ac.cn

4) Name: Jie Lv E-mail: lvjie@ms.giec.ac.cn

5) Name: Shili Lin E-mail: linsl@ms.giec.ac.cn

6) Name: Ziping Feng E-mail: fengzp@ms.giec.ac.cn

7) Name: Yongliang Li E-mail: y.li.1@bham.ac.uk

8) Name: Yulong Ding E-mail: Y.Ding@bham.ac.uk

Highlight:

2D network equivalent circuit considers the interplay of cell units.

The temperature non-uniformity Φ of multilayer model is bigger than that of lumped model

The temperature non-uniformity is quantified and the reason of non-uniformity is analyzed.

Increasing the thermal conductivity of the separator can effectively relieve the heat spot effect of ISC

Abstract: As the electrical and thermal characteristic will affect the batteries' safety, performance, calendar life and capacity fading, an electro-thermal coupled model for pouch battery $LiFePO_4/C$ is developed in normal discharge and internal short circuit process. The battery is discretized into many cell elements which are united as a 2D network equivalent circuit. The electro-thermal model is solved with finite difference method. Non-uniformity of current distribution and temperature distribution is simulated and the result is validated with experiment data at various discharge rates. Comparison of the lumped model and the multilayer structure model shows that the temperature non-uniformity Φ of multilayer model is bigger than that of lumped model and shows more precise. The temperature non-uniformity is quantified and the reason of non-uniformity is analyzed. The electro-thermal model can also be used to guide the safety design of battery. The temperature of the ISC element near tabs is the highest because the equivalent resistance of the external circuit (not including the ISC element) is the smallest when the resistance of cell units is small. It is found that increasing the thermal conductivity of integrated layer can effectively relieve the heat spot effect of ISC.

Keywords: Lithium ion battery; Electro-thermal coupled model; temperature distribution; internal short circuit

1. Introduction

Lithium ion batteries with its high specific energy, high theoretical capacity and good cycle-life are gaining popularity for Electric Vehicles (EVs) and Hybrid Electric Vehicles (HEVs) applications. However, a series of fire accidents indicate that thermal safety is still challenge to be overcome [1]. Thermal issue such as uneven temperature profile of batteries or high heat generation will make a great difference to its safety, performance, calendar life and capacity fading[2, 3]. Little non-uniformity of temperature can lead to great inconsistency of batteries. The inconsistency of batteries can do great harm to the performance of battery packs. Moreover, thermal runaway induced by internal short circuit (ISC) may lead to fire explosion. Therefore, thermal management system (TMS), which aims to optimize the performance by controlling the temperature distribution and to prevent the thermal runaway by controlling the heat transfer, is required.

Many literatures have investigated the thermal behavior of batteries and tried to predict the heat generation with different methods. A general heat source model [4] approved by D. Bernardi, was widespread used. The model divided the heat source into several terms including heat from reaction of electrochemical, heat from mixing, heat from phase change and joule heating. Other heat source models developed including electrochemical-thermal model and electro-thermal model. Electrochemical-thermal model based on porous electrode theory and Fick's law is used to describe electrochemical process and the mechanism of change of heat generation [5-10]. Electrochemical model is precise but it depends much on the parameter which is quite hard to measure. Also it is

hard to solve the complicated partial differential equations of the electrochemical model. The precision will decline in large format battery with 1D electrochemical model because it neglects the interplay of other cell elements in X-axis and Y-axis (figure 1). However, a 2D network equivalent circuit method can take it into account. Moreover, electro-thermal model based on 2D network equivalent circuit is simple and the parameter is easy to measure [1, 11-14]. It uses impedances or run time based model to represent the characteristics of the batteries [13].

$LiFePO_4$ electrode with olivine structure is a promising candidate electrode material because of its low price and high safety performance. Ahmadou Samba [15] developed a 2D thermal model to predict the temperature distribution but it did not consider the current distribution. M. Xu [9] used a pseudo 3D electrochemical-thermal model to describe the thermal behavior but it ignored the layer structure of pouch battery. C. Veth [14] used 3D electro-thermal model to simulate the current density and temperature distribution but the cause of non uniform distribution was not fully discussed and relation between temperature and property was implicit. Li Teng [16] separated the battery into several layers but the current density was implicit and the effect of multi-layer was not discussed.

Besides the prediction of temperature distribution, many literatures and patents have tried to predict and detect the internal short circuit (ISC) as it will generate a great amount of heat in a short time [17]. If the heat is not dissipated efficiently, the battery temperature will exceed a critical point, above which the electrolyte, active materials, and SEI (solid electrolyte interface) film will decompose, and eventually thermal runaway and even fire will take place [17]. Nail penetration experiment is often used to study the performance of ISC [17-18]. However, the fact that ISC probably occurs in a single cell unit (figure 1) is different from nail penetration

experiment in which the whole battery is penetrated. 1D Electrochemical model is excellent to study the mechanism of ISC [18-19] but it neglects the interplay between the short spot and the other parts of battery.

The pouch battery can be divided into many layers as illustrated in figure 1. Cathodes and anodes are coated in aluminum and copper foils. The property of each layer is different and the calculation of temperature distribution is not precise when we ignore the layer structure and the current distribution.

In this work, a multi-layer 3D thermal model is developed to simulate the temperature distribution of the battery while a 2D network equivalent circuit is developed to calculate the heat source. Detailed study of the thermal behavior of the battery during normal discharge and ISC process is discussed.

2. Model

A pseudo 3D electro-thermal model for a single $LiFePO_4$/graphite battery is developed based on a 2D network equivalent circuit and energy conservation. The nominal capacity is 20 Ah. The size of the pouch battery is 170 mm × 230 mm × 7 mm (width × length × thickness). The thickness of positive current collector (aluminum foil) is 20 μm while the thickness of negative collector (copper foil) is 14 μm. As illustrated in figure 1, we integrate positive electrode, separator and negative electrode as one integrated layer because the thermal property of separator and active material is much different from the current collector layer. The thickness of integrated layer is 140 μm. Cathodes and anodes are coated in aluminum and copper foils. We found that the battery contains 17 aluminum foil sheets, 16 copper foil sheets and 32 integration sheets after the

disassembly. As one cell unit is combined with one aluminum foil layer, one integration layer and copper foil layer, one pouch battery is combined with 32 cell units connected in parallel. That means a battery can be assumed as a "cell unit module".

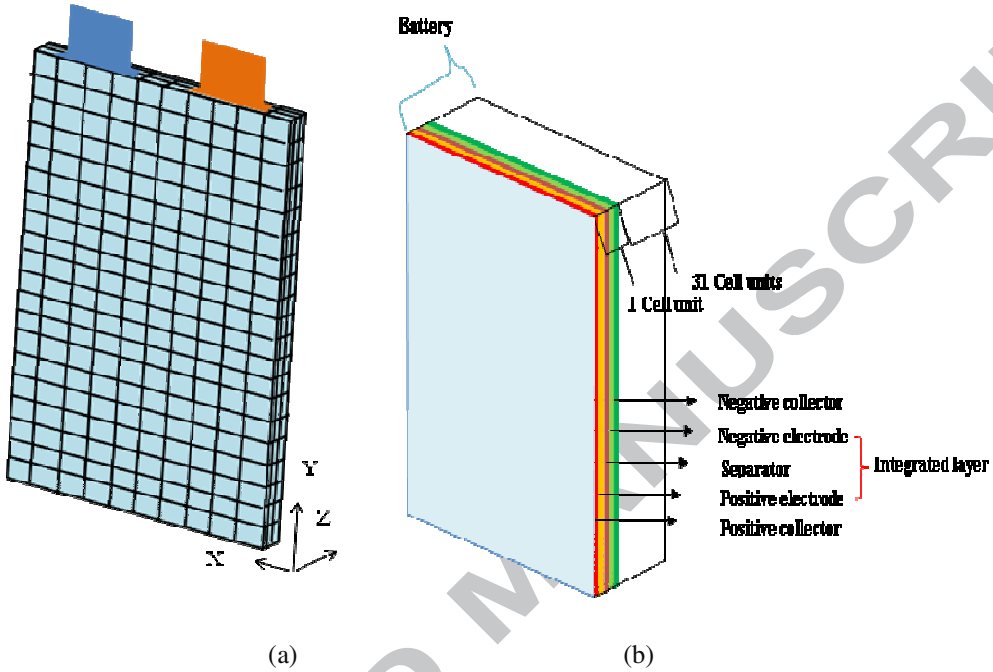

(a) (b)

Figure 1 Layer structure of pouch battery (the ratio of size is adjusted for better illustration)

2.1 Thermal model

For a pouch battery, the heat transfer should follow the energy conservation law:

$$\rho c \frac{\partial T}{\partial t} = \lambda \nabla^2 T + q \qquad (1)$$

where ρ is the density, c is heat capacity, λ is the heat conductivity, T is the temperature, t is time and q is the heat source. q is the summation of all the heat generations. We neglect the heat of phase change so that the heat generation includes there terms:

$$q = q_J + q_p + q_r \qquad (2)$$

where q_J is the joule heat, q_p is the irreversible electrochemical reaction heat and q_r is the reversible

entropic heat. If the electrochemical reaction is ideally reversible, the thermodynamic equation under a constant temperature T and constant pressure yields the following relation[20]:

$$\Delta G = \Delta H - T\Delta S \tag{3}$$

where the equation indicates the residual energy of reaction enthalpy change ΔH and electrical work (ΔG=-nFE_e) is released as heat energy q_r. And the reversible heat is described as:

$$q_r = T\Delta S \frac{I}{nF} \tag{4}$$

$$\Delta S = \frac{\partial \Delta G}{\partial T} = nF \frac{\partial E_e}{\partial T} \tag{5}$$

where I is the charge/discharge current, F is Faraday constant, E_e is the cell potential for open-circuit and n is the charge number pertaining to the reaction. We can get the value of $\partial E_e/\partial T$ from empirical equation or through the experimental data[11, 21]. The acquisition of q_J and q_p is described in electrical model in the next section.

Noting the convective heat transfer and radiation heat transfer on the boundary, we get equation (6)

$$\begin{aligned} q_s &= (h_{conv} + h_{rad})(T - T_{am}) \\ h_{rad} &= \varepsilon\sigma(T^2 + T_{am}^2)(T + T_{am}) \end{aligned} \tag{6}$$

where h_{conv} is the convective heat transfer coefficient, h_{rad} is the radiation heat transfer coefficient, T_{am} is the ambient temperature, ε is surface emissivity, and σ is the Stefan-Boltzmann constant.

The tabs are considered and the heat is conducted to the electrodes according to Fourier law of heat conduction.

2.2 Electrical model

A 2D network equivalent circuit is used in order to take the interplay of different cell

elements into consideration. The interplay is overlooked in 1D electrochemical model. One pouch battery is combined with 32 cell units connected in parallel. One cell unit can be discretized into many volume elements. Each volume element is regarded as a small cell element. When the volume element is small enough, it can be assumed that the temperature of that element is uniform. On the other hand, the volume element could not be too small because it should be large enough to represent the average value of a cell element. Therefore, we divide one cell unit into 20x10=200 cell elements and one pouch battery is connected by 20x10x32=6400 cell elements as illustrated in figure 1. The equivalent circuit[22] model of a complete battery is spatialized to 2D network model as illustrated in figure 2. According to the double electrode layer theory, the diffusion layer of $LiFePO_4$ battery is obvious enough to use a second order model[23]. The second order model contains V_{OCV} (open circuit voltage), polarization resistance R_p (including electrochemical polarization resistance R_{ep} and concentration polarization resistance R_{cp}), polarization capacitances (C_{ep} and C_{cp}), and ohmic resistances (R_0, $R_{ta,A}$, $R_{ax,A}$, $R_{ta,C}$ and $R_{ax,C}$). The parameters are depended on the temperature, SOC (state of charge) and rate of charge/discharge. The V_{OCV} of each cell element is almost the same to the V_{OCV} of the battery because the equilibrium potential is determined by the material of electrode/ electrolyte, concentration and temperature according to the Nernst equation. Eight resistances on the top and the bottom denote the positive current collector and negative current collector. The resistances on the current collector of each cell element are connected to the corresponding resistances of the adjoining cell element but the polarization resistances of each cell element are relatively independent from each other. All the cell elements in one cell unit are connected as a network. The resistances on the current collector are determined by the geometry and the material.

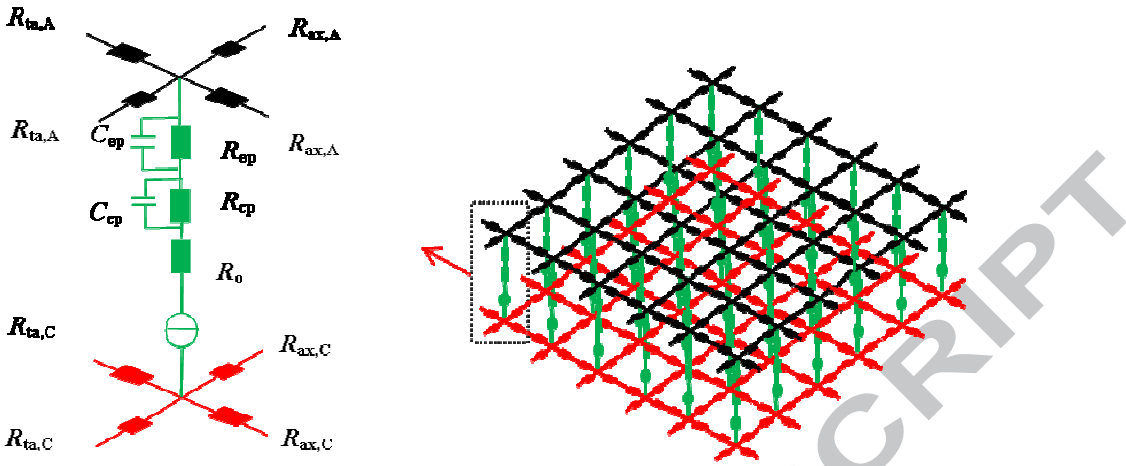

(a) (b)

Figure 2 Illustration of the cell element equivalent circuit (a) and 2D network equivalent circuit. Polarization capacitances are not illustrated for better visualization (b)

One pouch battery is connected by 32 cell units in parallel and it is assumed that the current between different cell units (not cell elements) is independent. It is rational in normal discharge process because the resistance and the current distribution in each cell unit are almost the same. We suppose that the current is divided into 32 parts equally and each part will flow into one cell unit. Every current collector except two at the edge will undertakes the currents generated by integrated layers on both sides. Then, we just need to focus on the grid circuit combined with 20x10=200 cell elements in one cell unit. What we concern about is the current in each circuit branch. Based on the Kirchhoff's current law, the sum of currents flowing into a node is equal to the sum of currents flowing out of that node.

$$\sum_{k=1}^{m} I_k(T, SOC) = 0 \qquad (7)$$

where the I_k is the branch current flowing in or out of the node. According to the Kirchhoff's voltage law, the directed sum of the electrical potential differences (voltage) in a closed loop is zero.

$$\sum_{k=1}^{m} V_k(T, SOC) = 0 \tag{8}$$

where m is the total number of electric elements in a closed loop and V_k is the voltage of the electric element (polarization resistances, resistances on the current collector and the power source). In discharge process, we acquire equation (9) from the second order model.

$$\begin{aligned} V_t(T, SOC) &= V_{ocv}(T, SOC) - I_k(T, SOC) \bullet R_o(T, SOC) - V_{ep}(T, SOC) - V_{cp}(T, SOC) \\ V_{ep}(T, SOC) &= I_k(T, SOC) R_{ep}(T, SOC) \bullet (1 - e^{-t/\tau_{ep}}) \\ V_{cp}(T, SOC) &= I_k(T, SOC) R_{cp}(T, SOC) \bullet (1 - e^{-t/\tau_{cp}}) \end{aligned} \tag{9}$$

where the τ_{ep} and τ_{cp} are the time constant which can be measure from experiment[23]. They almost remind unchanged in different temperature and SOC.

From all independent nodes and closed loop in the network, independent closed equations are list based on equations (7~9). We acquire the current in each branch after solving the equations. Therefore, for each cell element we can calculate the irreversible electrochemical reaction heat q_p and joule heat q_J.

$$q_J + q_P = \sum I_k^2(T, SOC) \bullet R_k(T, SOC) \tag{10}$$

where R_k (R_{ep}, R_{cp}, R_0, $R_{ta,A}$, $R_{ax,A}$, $R_{ta,C}$ and $R_{ax,C}$) is the corresponding resistance illustrated in figure 2 and I_k is the branch current flowing through R_k. In electrical model, temperature and SOC are input while the sum of irreversible electrochemical reaction heat and joule heat is output. The calculation of SOC is based on Ampere-Hour integral method.

2.3 Internal short circuit

As mentioned before, complex electrochemical reaction will occur and lead to thermal runway when the battery temperature exceeds a critical value[24]. The SEI film will melt and the electrolyte will decompose around 120 ^{o}C. That will lead to further reaction of the lithiated

graphite and the electrolyte [17, 24]. Therefore, we just focus on the ISC process before the temperature exceeds 150 ^{o}C. Major assumptions are described: no venting, no combustion, structurally intact; short remaining the same [25]. We suppose that the current is not limited by the mass transportation. In the process of ISC, the ISC resistance and the V_{OCV} will diminish [26]. In the electrical model, we replace the resistance R_{cp} R_{ep} and R_{oh} (figure 2) with short resistance R_{short} at the short cell element.

We study the feature of anode-cathode short and anode-aluminum short of single cell unit. The anode-aluminum short is considered by some studies to be more dangerous as the resistance at the short spot is relatively low and lack of good heat dissipation [19]. We assume the resistance of an-al short is around 30mΩ while the resistance of an-ca short is 300mΩ according to the data of reference [27].

In normal discharge process, current in different cell units is independent but now it is dependent in internal short circuit process. The intact cell units are regarded as power source with internal resistance. Heat generation from ISC contains the heat from discharge and the Joule heat at short spot.

2.4 Parameter

The battery is divided into many layers and the property of each layer is different. It is assumed that the thermal property including specific heat capacity, thermal conductivity and density does not change with temperature. They are given in table 1.

Table 1 Thermal property of different layers of battery

	specific heat capacity /(J·kg^{-1}·K^{-1})	thermal conductivity /(W·m^{-1}·K^{-1})	density /(kg·m^{-3})
Aluminum foil layer	880	200	2700

Integrated layer[28]	2738	0.11	1615
Copper layer	384	375	8920

For the parameters in electrical model, the V_{OCV} (open circuit voltage) is measured with experiment. Resistance of battery includes polarization resistances (R_{ep} and R_{cp}) and total ohmic resistances (R_{ohm}). They are measured by chronopotentiometry method. The potential response is shown in figure 3 (a). During the discharging process, we cut down the current and measure the voltage of the battery at that transient state. The response of ohmic resistance is very fast and the response of polarization is lagging. They are given in equations:

$$R_{ohm} = \frac{U_a - U_b}{I}$$
$$R_{ep} + R_{cp} = \frac{U_a - U_c}{I} - \frac{U_a - U_b}{I} \quad (11)$$

The U_a, U_b, and U_c are shown in figure 3(a). The experiment data is illustrated in figure 3 (b). Noticing that the ohmic resistance reminds nearly unchanged, it means the result is rational. Besides the method we used, it is reasonable to measure the resistances with the electrochemical impedance spectroscopy (EIS).

Of course, the resistances measured from the experiment belong to the whole battery. Therefore, they should be transferred to the cell elements' resistances based on the aforementioned electrical model. Collector resistances are calculated based on material and geometry. The ratio of R_{po}, R_c and R_{ohm} is fixed and the ratio value is based on the measure. Anyway, in constant-current discharge mode, the ratio is not so important in thermal calculation because the sum of these resistances is nearly invariable after 100 s discharging according to equations (9).

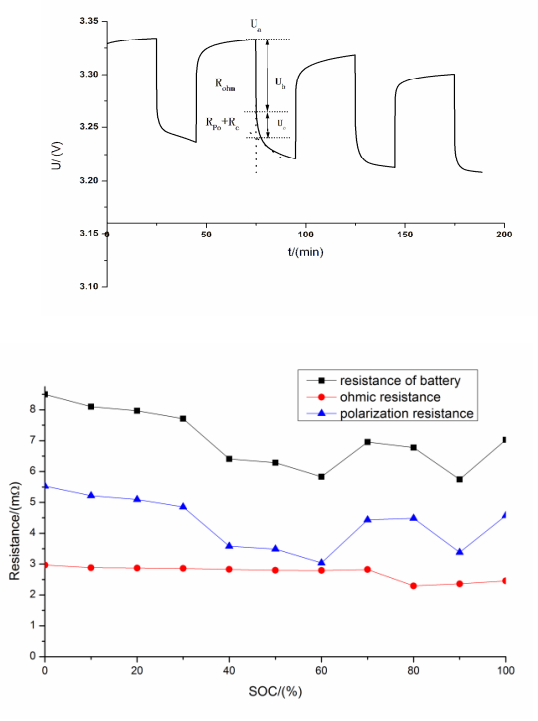

(a) (b)

Figure 3 The potential response of battery (a) and resistance of battery (b) measured with chronopotentiometry method

2.5 Solution of equations

As mentioned before, a pouch battery contains 17 aluminum foil layers, 16 copper foil layers and 32 integration layers. A cell unit is discretized into 20x10 cell elements in electrical model. Therefore, in the thermal model the pouch battery is discretized into 20 x 10 x (17+16+33) = 13200 volume elements correspondingly. The control equation and the boundary condition equations are described in the aforementioned thermal model while the heat source term can be acquired from electrical model. Then, the finite difference method is used to solve the partial differential equations.

In the thermal model solution, the number of the equations is large and the nonzero element

in the coefficient matrix is sparse. Therefore we use Gauss–Seidel method for the iterations. In the electrical model, we use Gaussian elimination method to solve the equations. We note that the change of temperature from thermal model would influent the parameter of electrical model while the change of electrical model would influent the generation of the thermal model. In order to decouple, the temperature used in the electrical model comes from the thermal model at the last moment. The flowchart can be seen in figure 4. The calculation procedure is written in C language by ourselves and run in Linux operation system.

Result of finer grid (30 x 20 x (17+16+32) = 39000 volume elements) is compared with the coarse grid (20 x 10 x (17+16+32) = 13000 volume elements). The difference of simulated temperature is below 3% . That means the grid is fine enough with 20 x 10 (17 + 16 +32) = 13000 volume elements.

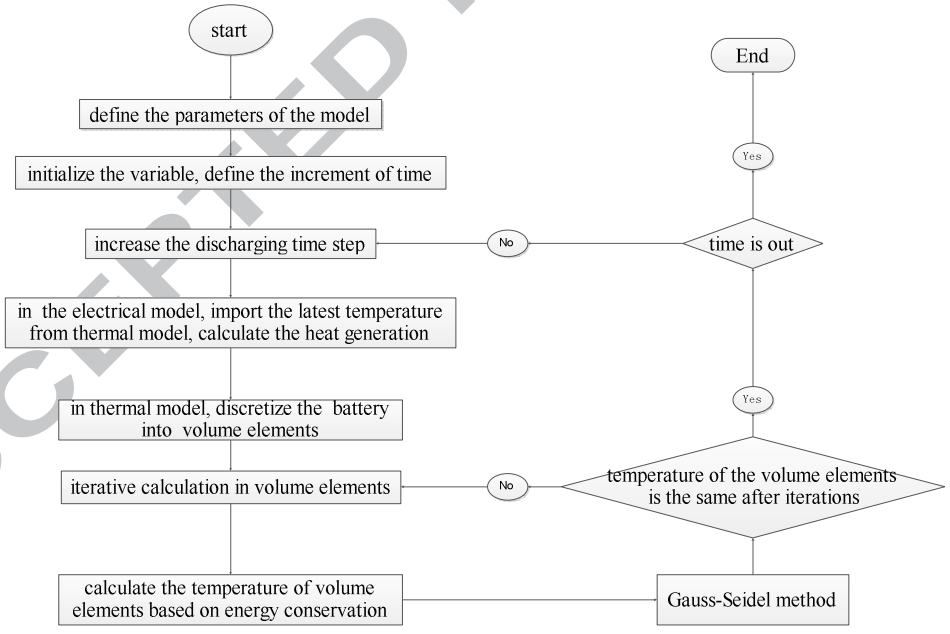

Figure 4 The flowchart of solution

3 Validation of model

3.1 Experimental validation of model

A commercial pouch battery (capacity 20Ah, nominal voltage 3.2V) was experimentally tested. The resistance was measured with chronopotentiometry method and the result was illustrated in figure 3. The apparatus was described in reference [29] where the work was done by our team. The batteries are charged by LAND-CT2001B, which is a charge and discharge multi-channel testing and controlling system, and are discharged by a programmable electronic load ITECH-IT8516. The operating currents, voltages, and temperature are monitored by data acquisition modules Agilent 34970A, and then processed by a host computer with built in software for programming charge and discharge. The battery was discharge at constant-current until it reached the cut-off voltage 2.7V. In order to validate the temperature field of the battery during discharging process, eight K-type thermocouples were placed on the front surface of the battery.

Figure 5(a) shows excess temperature profile at the point # 3 obtained by experiment and simulation at various discharge rate (0.5 C, 1.0 C, 1.5 C, 2.0 C. Here, the discharge rate C is equal to current of discharge divided by nominal capacity). Simulation results agree well with experiment. The excess temperature at high discharge rate increased faster because the heat generation is higher. Compared to the excess temperature at point #1and point #2 illustrated in figure 6(b), prediction for point #3 is more precise with this model. That is because temperature at point #1 and point #2 is more susceptible to the tabs. The temperature of tabs is sensitive to contact resistance and ambient environment. The small deviation between the experiment and the simulation is due to the reversible heat which is gotten from the reference [11] during the calculation. Though the change trend of reversible heat is similar, there exits small deviation in

different references [30]. The calculation result may improve if the reversible heat was obtained from experiment with the same type of battery. Other reason is that the convective heat transfer coefficient is not precisely estimated. We assume the convective heat transfer coefficient is around 4W/m2 under natural convection. The result will be better if the experiment is conducted under adiabatic condition.

The figure 5(b) illustrates the voltages of the battery at 1C discharge rate in simulation and experiment. They agree well with each other. The deviation at the beginning is bigger, relatively. That may be because the actual polarization resistance of battery is small than expected. At the beginning of discharge, the concentration gradient of Li+ is small and changes fast relatively. That may bring error to the result as the chosen step of the measure is a little bigger.

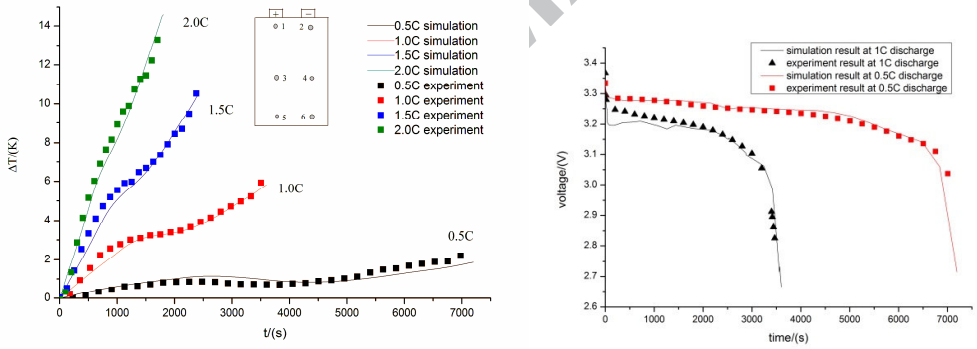

(a) (b)

Figure 5 (a) comparison of simulated results of average surface temperatures at point #3 with experimental data during galvanostatic discharge (0.5 C, 1.0 C, 1.5 C, 2.0 C). (b) voltage curve at 1 C (0.5 C) discharge

Temperature distribution was measured with K-type thermocouples at various rate of discharge. As illustrated in figure 6, 6 thermocouples were placed on the surface of the battery while two were placed on the tabs. Figure 6 shows the comparison of surface excess temperature

of different point during galvanostatic discharge (1 C, 2 C) under natural convection condition. An acceptable agreement of simulation and experimental curves can be seen. The deviation of simulation and experiment at point #1and point #2 is bigger especially at 2 C discharge rate. This may be attributed to the influence of current collecting tabs. Temperature of positive tab is much higher than the battery. Convective condition and touch resistance can make a big difference to the temperature of tabs. Another reason is probably the effect of lateral current which is not rigorously considered in this model. The lateral current will flow to the tabs through the electrodes, not the current collectors[31].

The non-uniform of temperature distribution is quite serious especially in high discharging rate. At 2C discharge rate, the difference between the maximum and the minimum is as high as 14K, which would do great harm to the performance of the battery. Lifetime of battery will decrease seriously with so large temperature deviation. The temperature deviation will aggravate in battery modules because of uneven cooling condition. Therefore, necessary measurements should be taken to control not only the temperature but also the temperature non-uniformity of the battery.

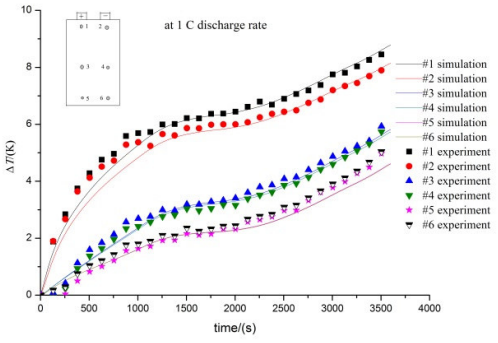

(a)

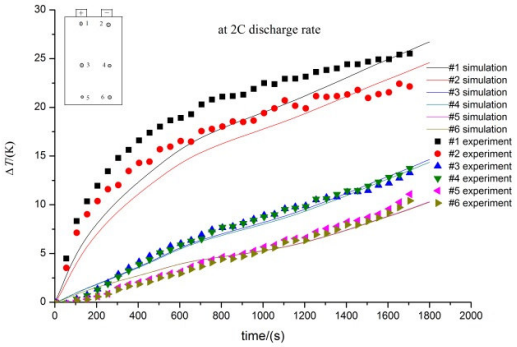

(b)

Figure 6 Comparison of surface excess temperature of different point during galvanostatic discharge (1C on the picture a, 2C on the picture b) under natural convection condition. The simulated data is smooth while the experiment data is fluctuant

From the comparison of temperature curve, the slope at the middle stage (from SOC = 35% or t = 1260 s to SOC = 70% or t = 2520 s) is gentle at 1C discharge rate but it is steep at 2 C discharge rate. This is attributed to the influence of reversible heat which contributes more than 50% of the total heat generated (in Joules) at low discharge rate[32]. Reversible reaction heat is endothermic during discharging process and changes with SOC.

The model can also be used to calculate the temperature distribution and current density distribution during charge process. We just need to change the reversible heat as heating effect is different in the two processes (discharge and charge).

3.2 Comparison of two models

The model is convincing to predict the temperature field of the pouch battery when resistance is precisely measured and working condition is well described. The electro-thermal model is multilayer model as described before. Compared to the lumped model in which the thermal property of all layers is equal to the same equivalent value, the multilayer model well describes the inner structure of battery. Equivalent method for equivalent property is described in reference [28] in which the work was done by our team with the same type of battery. The simulation result of two models (lumped model and multilayer model) and the experiment result are shown in figure 7. According to the definition of irradiance uniformity in reference [33], temperature non-uniformity is defined as the ratio of deviation to the average temperature:

$$\phi = \frac{T_{cen,\max} - T_{cen,\min}}{T_{cen,\max} + T_{cen,\min}} \tag{12}$$

where the $T_{cen,\max}$ and $T_{cen,\min}$ are maximum and minimum centigrade temperature of battery. Φ is equal to zero when the temperature of battery is uniform. From the comparison of the simulated result, temperature is more uniform in lumped model than in multilayer model. The reason of large deviation is that the heat conductivity of copper foil and aluminum foil is two orders larger in magnitude than that of electrode material. Large discrepancy between different layers will make the equivalent heat conductivity inaccurate to calculate the temperature field. Besides, calculation of equivalent heat conductivity and equivalent specific heat capacity is always independent from each other. As a result, equivalent thermal diffusivity ($\lambda/\rho c$) is overestimated in lumped model. The temperature non-uniformity Φ of multilayer model is bigger than that of lumped model and shows more accurate. The analysis and conclusion can be extended to cylindrical battery because its inner physical structure is the same to pouch battery.

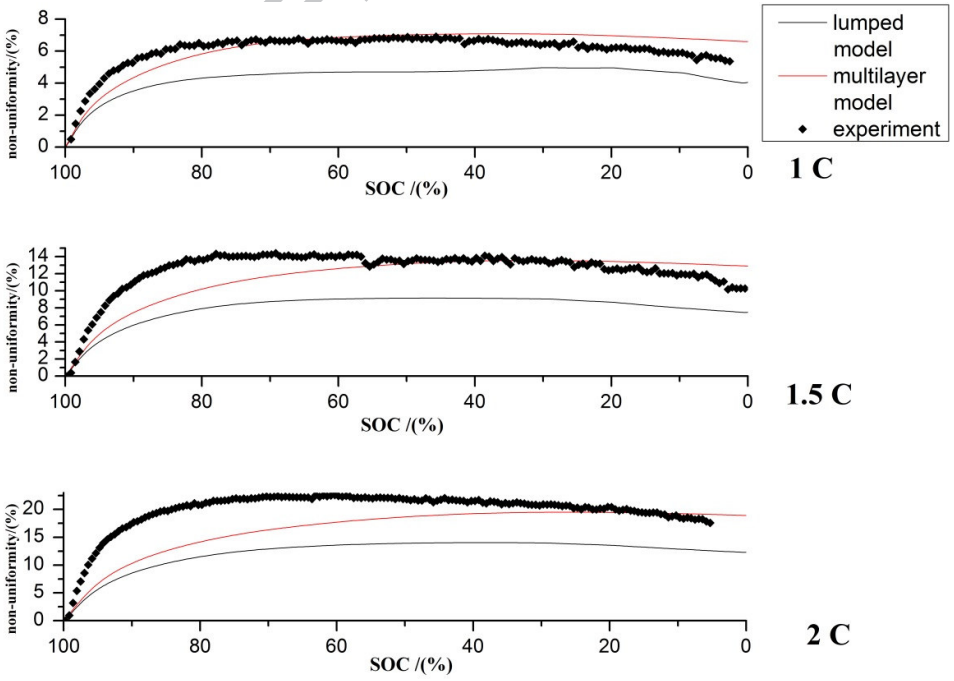

Figure 7 Comparison of temperature non-uniformity at various discharge rate (1 C, 1.5 C, 2 C)

4 Results and discussion

From the aforementioned description, the electro-thermal model is simple and the parameters are easy to measure. But the calculation result agrees with experiment.

4.1 Simulation result of temperature distribution

Numerical calculations were performed for the $LiFePO_4$/graphite pouch battery at 1 C, 2 C discharge rate to better understand the electrical and thermal characteristics of the battery. Figure 8 shows the excess temperature distribution in 3D cloud picture at 1 C discharge rate. The arrows indicate the direction and magnitude of the current flowing in the current collector layer of battery. Obviously the current flows into (out) the negative (positive) current collecting tab. The magnitude decreases with the increasing distance from the tab. That is because the local current flows across the electrodes of local cell element, then it will change the direction vertically and flows into the current collector[34]. All current from the local cell elements will gather in the tab. The current distribution is similar to the result of reference [9] and the model of reference [32].

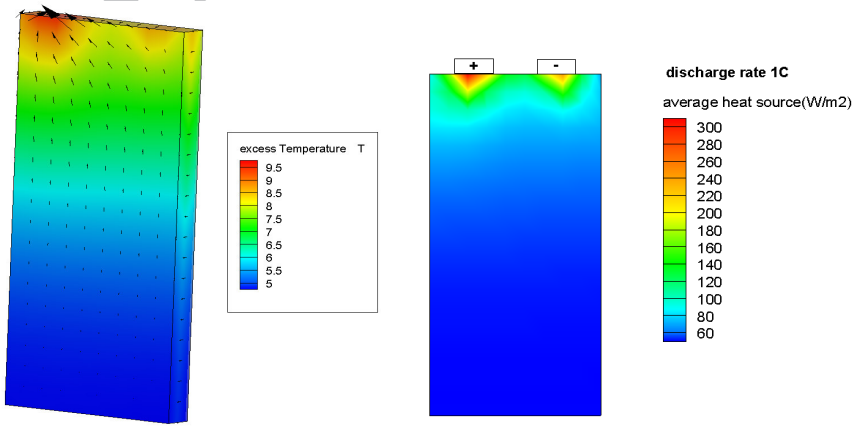

(a) (b)

Figure 8 The excess temperature distribution under 1 C discharge at the end of discharge (t = 3600s). The arrows indicate the direction and magnitude of the current. Tabs are not shown in the

picture. The ratio of x, y and z is adjusted (a). spatial distribution of average heat generation at 1C discharge rate (b)

From the excess temperature distribution in figure 8, the excess temperature near the tab is higher. The temperature near the positive current collecting tab (point #1 as illustrated in figure 5) is higher than the temperature near the negative tab (point #2). It is because the electrical conductivity of the aluminum foil is lower than that of the copper foil. Extra simulation result have proved that the temperature deviation of point #1 and point #2 was less than 0.1K at 1C discharge rate when the current collectors were the same material (copper foil or aluminum foil).

It is interesting to notice the non-uniform of temperature distribution. As illustrated in figure 8, temperature increases gradually from the bottom to the top of battery. The maximum excess temperature is 8.7 K while the minimum is 4.6 K. The main reason is that the resistance of collectors and uneven current distribution will lead to non-uniform distribution of local voltage (U_{local}) of cell elements, which will lead to non-uniform of overpotential distribution. Figure 9 shows the overpotential of local cell elements at the beginning of 1 C discharging. Generally, a greater overpotential will drive the electrochemical reaction of the electrode at a faster rate, which will lead to more electrochemical reaction heat[9]. The distribution of average heat generation at 1C discharge rate in figure 8(b) is quite similar to the distribution of overpotential in figure 9(a). The overpotential near the tabs is larger. The distribution is similar to temperature distribution. The overpotential of local cell element is determined by equation (13):

$$\eta_{local} = U_{eq,local} - U_{local} \tag{13}$$

The open circuit potential of the local cell element $U_{\text{eq,local}}$ depends on temperature, SOC and material of electrode/ electrolyte. At the beginning of discharging, the open circuit potentials of

the local cell elements are equal. The working voltage of local cell element U_{local} is determined by the electrical 2D network model built in section 2.2. Both the variation trend and the magnitude of overpotential in figure 8 is similar to that in the reference[9] .

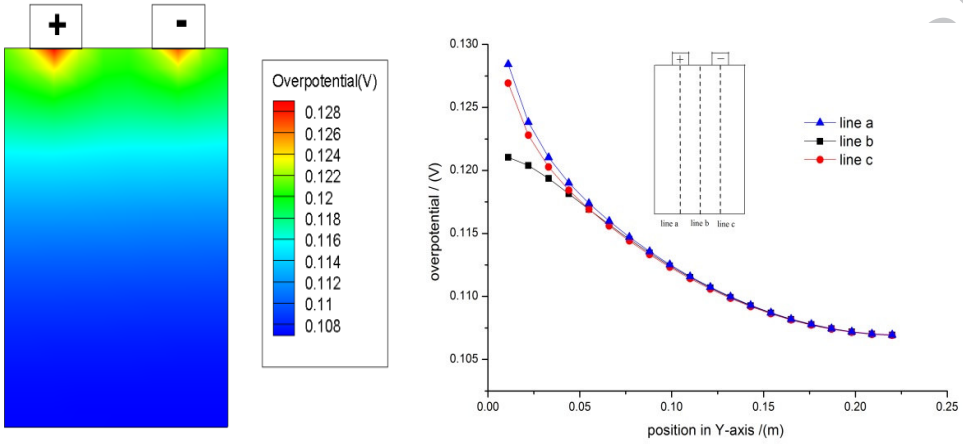

(a) (b)

Figure 9 The overpotential distribution of local cell elements at the beginning of 1 C discharging. The distribution on the x-y plane (a) and the distribution along the a line (b)

4.2 Internal short circuit

The multilayer electro-thermal model can also be used to simulate the thermal behaviour of ISC before the battery temperature reaches 150°C. We just study the situation where the battery is under the condition of open circuit. Firstly, ISC at different state of charge (SOC) was simulated and we found that temperature of battery with higher SOC was higher, relatively. That was similar to the result of literature [35].

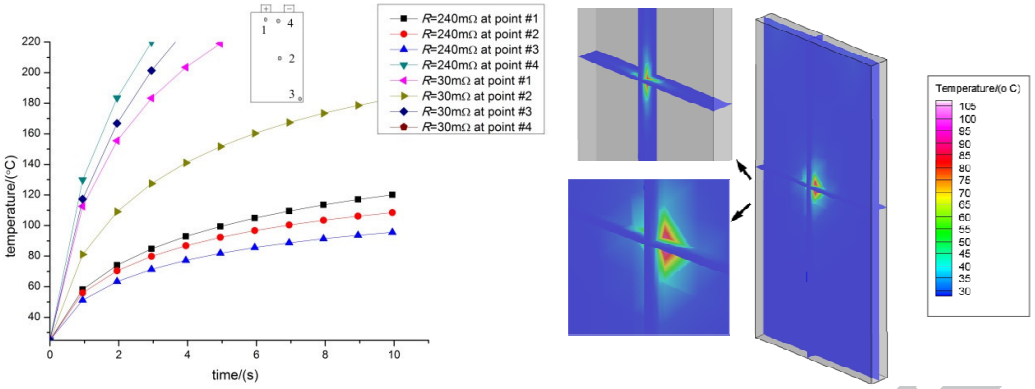

(a) (b)

Figure 10 (a) Temperature of short-circuit cell element (anode-cathode short or anode-aluminum short) at different position. (b) Temperature distribution (t = 10 s) of battery suffering anode-cathode short at the middle position of the middle cell unit layer

Internal short circuit in a single cell unit is studied. We assume that one cell element in the middle cell unit (the 16th integrated layer and the adjoining collector layers) is short. Temperature of short-circuit cell element (anode-cathode short or anode-aluminum short) at different position is calculated and shown in figure 10(a). We assume the resistance (R_{short}) of the an-ca short-circuit cell element is 240 mΩ while that of the an-Al short-circuit cell element is 30 mΩ [36]. The change trend is similar to that in the literature [36]. It can be seen that the an-Al short has a higher risk of thermal runaway when only a single layer is short. The result shows the same trend as described in the literature [19]. An-ca short will not go to thermal runaway though its temperature is higher than that at normal discharge. Temperature of short-circuit cell element at different position is different as illustrated figure 10(a). When the ISC cell element is near the tabs (#1), the spot temperature is the highest because of the influence of the collector resistance and the other cell units (different layers). Taking all cell elements (both from the short cell unit and the normal cell units) into consideration, the network circuit can be regarded as simple series circuit

connected with one short cell element, one equivalent resistance and one power source. Based on Thevenin's theorem, the equivalent resistance of the external circuit (not including the short cell element) can be calculated through the network model built in section 2.2. It is found that the equivalent resistance is the lowest when the #1 cell element is short. That means the voltage loss is the lowest in this way, which would lead to highest short current. Extra simulation also showed that the temperature of the (#4) short cell element at the middle of two tabs is the highest when the internal resistance of cell units becomes larger enough. That is because the equivalent resistance will become the lowest at (#4) short cell element if the internal resistance of cell units increases. From figure 10(a), temperature difference of an-Al short-circuit cell element at different position is larger than that of an-ca short-circuit cell element. That may be because magnitude of the short resistance of an-Al short is closer to that of collector resistance, relatively. As a result, an-Al short is more sensitive to the position. Another reason may attribute to the high current in an-Al short which can lead to high temperature.

Temperature distribution (t = 10 s) of battery suffering anode-cathode short at the middle position of the middle layer is illustrated in figure 10. Temperature difference between the middle layer and the surface is as high as 55 K and that would make the detection of the ISC process difficult. The main reason is the low thermal conductivity of separator ($k \approx 0.1$ $W \cdot m^{-1} \cdot K^{-1}$) and electrode ($k \approx 1$ $W \cdot m^{-1} \cdot K^{-1}$) [9]. Through the simulation, the temperature of an-ca short and an-Al short element at middle layer/surface (t = 10 s) is shown in table 2. The temperature of short element at the middle layer is the highest in the battery. It is found that increasing the thermal conductivity of integrated layer especially the separator layer can effectively relieve the heat spot effect of ISC. Moreover, increasing the thermal conductivity will make the detection of ISC easier.

Table 2 The temperature of an-ca short and an-Al short element at middle layer/surface (t = 10 s)

thermal conductivity of integrated layer/($W \cdot m^{-1} \cdot K^{-1}$)	0.45	1	10
Temperature of an-ca short element at the middle/surface /(^oC)	72/26	56/29	37/34
Temperature of an-Al short element at the middle/surface /(^oC)	150/28	99/36	60/51

Thermal behaviour of two ISC cell elements is simulated. When the two spots lie in the same cell unit, the heat generation increases but the highest temperature depends on the position of the two spots. The highest temperature will decrease if the distance of two spot is not close. That may be because the current is divided into two parts and the heat generation decreases at the spot. When the two spot lie in the same position of adjacent cell unit, the highest temperature would increase fast. Through simulation, the battery may go to thermal runaway if three adjacent cell units are an-ca short. Penetration experiment easily leads to fire because all cell units are short. The heat generation of nail penetration is much depending on the ISC resistance and contact resistance.

As we can see, the electro-thermal model can guide the safety design of battery. It would get high precision if the variation of ISC resistance is defined.

5 Conclusion

An electro-thermal coupled model for pouch battery is developed to study the thermal performance during normal discharge and internal short circuit process. The battery is discretized into many cell elements which are united as a 2D network equivalent circuit. The thermal model takes the multilayer structure into consideration.

The electro-thermal coupled model is validated with experiment and the simulation result can predict the temperature distribution of pouch battery. The temperature non-uniformity Φ of

multilayer model is bigger than that of lumped model and shows more accurate. That is because equivalent thermal diffusivity ($\lambda/\rho c$) may be overestimated when calculation of equivalent heat conductivity and equivalent specific heat capacity is independent from each other.

Current density distribution and excess temperature distribution are simulated with the model. The temperature non-uniformity is quantified and the reason of non-uniformity is analyzed. It is observed that non-uniformity of temperature distribution is large in the battery and it will aggregate with the discharge rate increasing. Non-uniform temperature distribution is attributed to the resistance of collectors and the uneven distribution of current density.

The electro-thermal coupled model is also used to study the performance of ISC and guide the safety design of battery. The temperature of the ISC element near tabs is the highest because the equivalent resistance of the external circuit (not including the ISC element) is the smallest when the resistance of cell units is small. It is also found that increasing the thermal conductivity of integrated layer can not only effectively relieve the spot effect of ISC but also make the detection of ISC easier.

Abbreviation

c heat capacity
E_e cell potential for open-circuit
F Faraday constant
h_{conv} convective heat transfer coefficient
h_{rad} radiation heat transfer coefficient
I charge/discharge current
I_k branch current flowing in or out of the node
n the charge number pertaining to the reaction
q total heat source
q_J joule heat

q_p irreversible electrochemical reaction heat
q_r the reversible entropic heat
R_{cp} concentration polarization resistance
R_{ep} electrochemical polarization resistance
R_{ohm} total ohmic resistances (including R_o, $R_{ta,A}$, $R_{ax,A}$, $R_{ta,C}$ and $R_{ax,C}$)
R_p polarization resistance
R_{short} resistance of internal short circuit
t time
T temperature
T_{am} ambient temperature
$T_{cen,max}$ maximum centigrade temperature of battery
$T_{cen,min}$ minimum centigrade temperature of battery
V_k the voltage of the electric element
$U_{eq,local}$ open circuit potential of the local cell element
U_{local} working voltage of local cell element
τ_{ep} time constant
τ_{cp} time constant
ρ density
λ heat conductivity
ε surface emissivity
σ Stefan-Boltzmann constant
Φ temperature non-uniformity
η_{local} overpotential of local cell element
ΔH reaction enthalpy change
ΔG electrical work

Acknowledge

The authors would like to thanks for supports by National Natural Science Foundation of China [grant numbers No.51477171, No.5151101411]; the Guangdong Science and Technology Project for International Cooperation [grant number 2015B050501008]; the Guangzhou Science and Technology Project [grant number 201509010018] and the Youth Innovation Promotion Association of CAS [grant number 2013230].

References

[1] Saw LH, Ye Y, Tay AAO. Electro-thermal analysis and integration issues of lithium ion battery for electric vehicles. Applied Energy. 2014;131:97-107.

[2] Li Z, Lu L, Ouyang M, Xiao Y. Modeling the capacity degradation of LiFePO4/graphite batteries based on stress coupling analysis. Journal of Power Sources. 2011;196:9757-66.

[3] Sarasketa-Zabala E, Gandiaga I, Rodriguez-Martinez LM, Villarreal I. Calendar ageing analysis of a LiFePO4/graphite cell with dynamic model validations: Towards realistic lifetime predictions. Journal of Power Sources. 2014;272:45-57.

[4] D B, E P, J N. A general energy balance for battery systems[J]. Journal of the electrochemical society. Journal of the electrochemical society. 1985;132:5-12.

[5] Jiang F, Zeng J, Peng P, He S. Direct Numerical Simulation Modeling of Multidisciplinary Transport during Li-Ion Battery Charge/Discharge Processes. Journal of Advanced Thermal Science Research. 2015;1:32-43.

[6] Lin C, Xu S, Li Z, Li B, Chang G, Liu J. Thermal analysis of large-capacity LiFePO4 power batteries for electric vehicles. Journal of Power Sources. 2015;294:633-42.

[7] Srinivasan V, Wang CY. Analysis of Electrochemical and Thermal Behavior of Li-Ion Cells. Journal of The Electrochemical Society. 2003;150:A98.

[8] Wu B, Yufit V, Marinescu M, Offer GJ, Martinez-Botas RF, Brandon NP. Coupled thermal–electrochemical modelling of uneven heat generation in lithium-ion battery packs. Journal of Power Sources. 2013;243:544-54.

[9] Xu M, Zhang Z, Wang X, Jia L, Yang L. A pseudo three-dimensional electrochemical–thermal model of a prismatic LiFePO4 battery during discharge process. Energy. 2015;80:303-17.

[10] l. J Zhang, W. B. Li, and H.Z. Cheng: coupled thermodynamic-electrochemical 3D FE model for single lithium-ion battery with consideration of uneven heat generation and temperature distribution. automotive engineering . 2015; 37(12): 1382-1389

[11] Fleckenstein M, Bohlen O, Roscher MA, Bäker B. Current density and state of charge inhomogeneities in Li-ion battery cells with LiFePO4 as cathode material due to temperature gradients. Journal of Power Sources. 2011;196:4769-78.

[12] Hu X, Li S, Peng H. A comparative study of equivalent circuit models for Li-ion batteries. Journal of Power Sources. 2012;198:359-67.

[13] Saw LH, Ye Y, Tay AAO. Electro-thermal characterization of Lithium Iron Phosphate cell with equivalent circuit modeling. Energy Conversion and Management. 2014;87:367-77.

[14] Veth C, Dragicevic D, Pfister R, Arakkan S, Merten C. 3D Electro-Thermal Model Approach for the Prediction of Internal State Values in Large-Format Lithium Ion Cells and Its Validation. Journal of the Electrochemical Society. 2014;161:A1943-A52.

[15] Samba A, Omar N, Gualous H, Firouz Y, Van den Bossche P, Van Mierlo J, et al. Development of an Advanced Two-Dimensional Thermal Model for Large size Lithium-ion Pouch Cells. Electrochimica Acta. 2014;117:246-54.

[16] T. Li, C. T. Lin, and Q. S. Chen: Lithium-ion battery 3-diemensional multi-layer multi-field model. J Tsinghua Univ (Sci & Tech). 2012; 52 (7): 995-1000 .

[17] Zhao R, Liu J, Gu J. Simulation and experimental study on lithium ion battery short circuit. Applied Energy. 2016;173:29-39.

[18] Zhao W, Luo G, Wang CY. Modeling Nail Penetration Process in Large-Format Li-Ion Cells. Journal of the Electrochemical Society. 2014;162:A207-A17.

[19] Fang W, Ramadass P, Zhang Z. Study of internal short in a Li-ion cell-II. Numerical investigation using a 3D electrochemical-thermal model. Journal of Power Sources. 2014;248:1090-8.

[20] Onda K, Ohshima T, Nakayama M, Fukuda K, Araki T. Thermal behavior of small lithium-ion battery during rapid charge and discharge cycles. Journal of Power Sources. 2006;158:535-42.

[21] Forgez C, Vinh Do D, Friedrich G, Morcrette M, Delacourt C. Thermal modeling of a cylindrical LiFePO4/graphite lithium-ion battery. Journal of Power Sources. 2010;195:2961-8.

[22] Fleckenstein M, Bohlen O, Roscher MA, Bäker B. Current density and state of charge inhomogeneities in Li-ion battery cells with LiFePO4 as cathode material due to temperature gradients. Journal of Power Sources. 2011;196:4769-78.

[23] W. Jiang. Research on the parameters of LiFePO4 power battery second-order RC model, PhD Dissertation, Zhejiang University. 2015.

[24] Yang H, Bang H, Amine K, et al. Investigations of the exothermic reactions of natural graphite anode for Li-ion batteries during thermal runaway. Journal of the Electrochemical Society, 2005, 152(1): A73-A79.

[25] Kim G H SK, Pesaran A. Lithium-Ion Battery Safety Study Using Multi-Physics Internal Short-Circuit Model. 2009.

[26] Ouyang M, Zhang M, Feng X, Lu L, Li J, He X, et al. Internal short circuit detection for battery pack using equivalent parameter and consistency method. Journal of Power Sources.

2015;294:272-83.

[27] Zhang C SS, Sprague M A. Representative-Sandwich Model for Mechanical-Crush and Short-Circuit Simulation of Lithium-ion Batteries. NREL. 2015.

[28] J. S. Lin, W.J. Song, R.S. Gao and Z.P. Feng: Study on thermo-physical property measurement and temperature rise characteristic of LiFePO4 power battery. Chinese Journal of Power Sources. 2015; 39:739-742

[29] Zhang Y, Song W, Lin S, Feng Z. A novel model of the initial state of charge estimation for LiFePO4 batteries. Journal of Power Sources. 2014;248:1028-33.

[30] Lin C, Xu S, Li Z, Li B, Chang G, Liu J. Thermal analysis of large-capacity LiFePO4 power batteries for electric vehicles. Journal of Power Sources. 2015;294:633-42.

[31] Kim US, Shin CB, Kim C-S. Modeling for the scale-up of a lithium-ion polymer battery. Journal of Power Sources. 2009;189:841-6.

[32] Viswanathan VV, Choi D, Wang D, Xu W, Towne S, Williford RE, et al. Effect of entropy change of lithium intercalation in cathodes and anodes on Li-ion battery thermal management. Journal of Power Sources. 2010;195:3720-9.

[33] Winston R, Fu L, Gordon JM, Leutz R, Annen HP. Secondary optics for Fresnel lens solar concentrators. 2010;7785:778509.

[34] Xu M, Zhang Z, Wang X, Jia L, Yang L. Two-dimensional electrochemical–thermal coupled modeling of cylindrical LiFePO4 batteries. Journal of Power Sources. 2014;256:233-43.

[35] Cai W, Wang H, Maleki H, Howard J, Lara-Curzio E. Experimental simulation of internal short circuit in Li-ion and Li-ion-polymer cells. Journal of Power Sources. 2011;196:7779-83.

[36] Volck T, Sinz W, Gstrein G, Breitfuss C, Heindl S, Steffan H, et al. Method for Determination

of the Internal Short Resistance and Heat Evolution at Different Mechanical Loads of a Lithium Ion Battery Cell Based on Dummy Pouch Cells. Batteries. 2016;2:8.

Table caption

Table 1 thermal property of different layers of battery

Table 2 The temperature of an-ca short and an-Al short element at middle layer/surface (t = 10 s)

Figure caption

Figure 1 Layer structure of pouch battery (the ratio of size is adjusted for better illustration)

Figure 2 Illustration of the cell element equivalent circuit (a) and 2D network equivalent circuit (b)

Figure 3 The potential response of battery (a) and resistance of battery (b) measured with chronopotentiometry method

Figure 4 the flowchart of solution

Figure 5 (a) comparison of simulated results of average surface temperatures at point #3 with experimental data during galvanostatic discharge (0.5 C, 1.0 C, 1.5 C, 2.0 C). (b) voltage curve at 1 C (0.5 C) discharge

Figure 6 Comparison of surface excess temperature of different point during galvanostatic discharge (1C on the picture a, 2C on the picture b) under natural convection condition. The simulated data is smooth while the experiment data is fluctuant

Figure 7 Comparison of temperature non-uniformity at various discharge rate (1 C, 1.5 C, 2 C)

Figure 8 The excess temperature distribution under 1 C discharge at the end of discharge (t = 3600s). The arrows indicate the direction and magnitude of the current. Tabs are not shown in the

picture. The ratio of x, y and z is adjusted (a). spatial distribution of average heat generation at 1C discharge rate (b)

Figure 9 The overpotential distribution of local cell elements at the beginning of 1 C discharging. The distribution on the x-y plane (a) and the distribution along the a line (b)

Figure 10 (a) Temperature of short-circuit cell element (anode-cathode short or anode-aluminum short) at different position. (b) Temperature distribution (t = 10 s) of battery suffering anode-cathode short at the middle position of the middle cell unit layer

Highlight:

2D network equivalent circuit considers the interplay of cell units.

The temperature non-uniformity Φ of multilayer model is bigger than that of lumped model

The temperature non-uniformity is quantified and the reason of non-uniformity is analyzed.

Increasing the thermal conductivity of the separator can effectively relieve the heat spot effect of ISC